VESICLES AND BIOMEMBRANES

REINHARD LIPOWSKY, *Max-Planck-Institut für Kolloid- und Grenzflächenforschung, Teltow-Seehof, Germany*

3-527-29476-7/98/$5.00 + .50

INTRODUCTION

The membranes and vesicles considered here are ultrathin and highly flexible sheets composed of lipids and other amphiphilic molecules (which have both a water-soluble, hydrophilic part and a water-insoluble, hydrophobic part). In biological systems, these membranes represent complex interfaces that partition space into different compartments and, thus, are responsible for the amazing architecture of these systems. One example of this architecture is shown in Fig. 1.

Biomembranes have been studied for a long time in biology, pharmacology, and medicine. On the micron scale, these membranes exhibit a unique combination of properties:

1. They form closed surfaces without edges;
2. they are highly flexible and, thus, can easily adapt their shape to external perturbations; and
3. in spite of this flexibility, they are rather robust and keep their structural integrity even for strong deformations.

This *combination of stability and flexibility* is a consequence of their molecular struc-

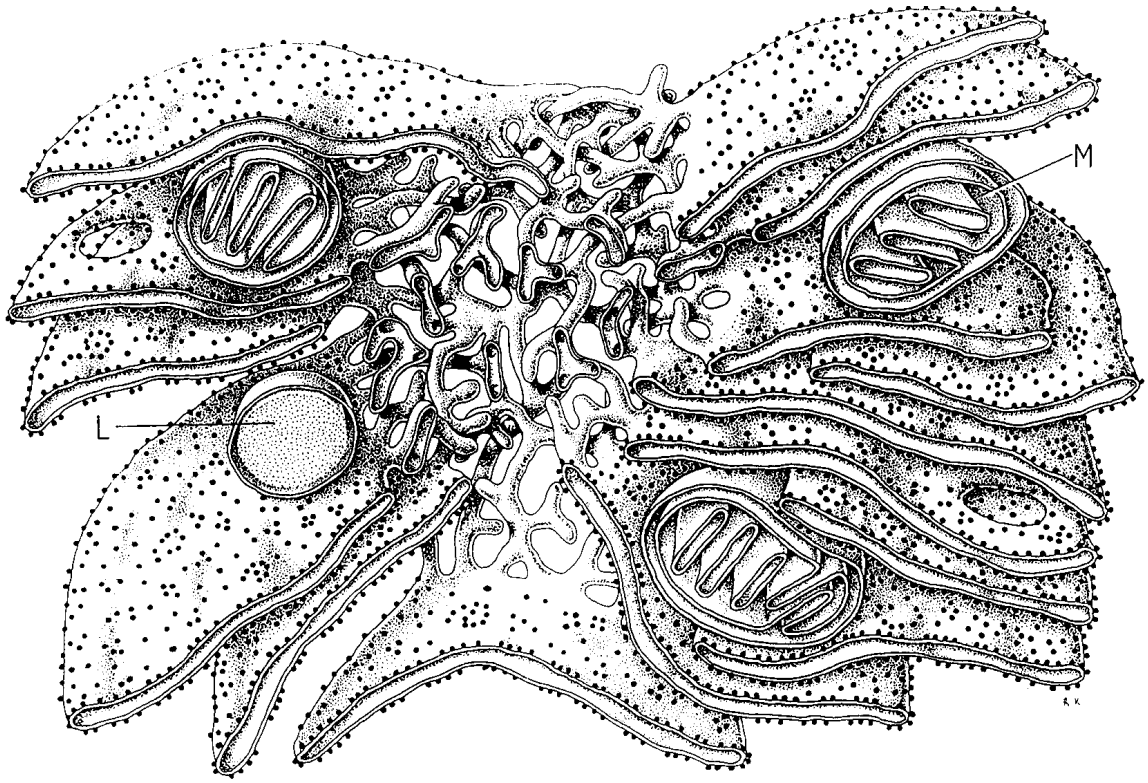

FIG. 1. Some internal membranes of a liver cell. The labyrinth of membrane sheets and tubes defines the endoplasmic reticulum; within the lamellar region, one sees the membranes of three mitochondria (M) and of one lysosome (L). (Krstic, 1976.)

ture. When viewed on the nanometer scale, each biomembrane consists of a specific mixture of many different amphiphilic molecules that reflect its diverse biological functions. However, in spite of this chemical complexity, all biomembranes are organized according to the same universal construction principle: their basic building block is provided by a *bilayer of lipid molecules.* The latter molecules are essentially *insoluble* in the aqueous solution, which ensures membrane stability. In addition, these lipid bilayers are maintained in a *fluid* state, which is the main mechanism underlying their enormous flexibility.

This article focuses on fluid bilayers that contain only one or a few lipid components. Even the simplest model membranes of this kind already exhibit several levels of *self-organization* that are reminiscent of biomembranes: The lipid molecules arrange themselves into bilayers; the bilayers spontaneously form closed bags or vesicles without edges; the vesicles adhere to one another and form various multilayer structures.

In addition, lipid bilayers in their fluid state can easily adapt to external forces by reorganization of their supramolecular structure. Indeed, one intriguing aspect of these membranes is their ability to undergo morphological changes: Depending on temperature and osmotic conditions, free membranes and vesicles exhibit a large variety of different shapes and shape transformations; similar shape changes can be induced by the formation of intramembrane domains; interacting membranes undergo transitions between bound and unbound states. A new level of self-organization is obtained when such bilayers are "decorated" with anchored polymers. These polymers form "mushrooms," "pancakes," or "brushes," which tend to curve the bilayers and to change their interactions.

Just like biomembranes, lipid bilayers are flexible but stable structures, which makes it possible to isolate them and to manipulate them in various ways: One can suck them into micropipettes, attach them to other surfaces, and grasp them with optical tweezers generated by focused laser beams. These bilayers can even tolerate local perturbations that lead to the formation of small holes: The bilayers restore their structural integrity since the holes close again spontaneously as long as the membranes do not experience a large lateral tension.

1. FROM CELLS TO VESICLES

1.1 Plasma Membrane and Internal Membranes

All living matter is built up from cells. Each cell is enclosed by its outer plasma membrane that controls the interaction between the cell and its environment. This applies both to the relatively small cells of bacteria or prokaryotes, which have no cell nucleus, and to the much larger cells of eukaryotes, which have such a nucleus. The latter class of organisms includes all animals and plants as well as single-celled microorganisms such as amoeba or yeast. In addition to the outer plasma membrane, all eukaryotic cells contain internal membranes that represent the boundaries of the internal organelles such as the nucleus, mitochondria, chloroplasts, etc. The membranes shown in Fig. 1, for example, represent the internal membranes that bound the endoplasmic reticulum and some mitochondria of a liver cell (Darnell *et at.,* 1990; Alberts *et al.,* 1994).

The total membrane area of an eukaryotic cell is relatively large. The membranes of a single liver cell, for example, have a total surface area of about $1.1 \times 10^5\ \mu m^2$ while its volume is about $5 \times 10^3\ \mu m^3$. About 98% of this large area belongs to the internal membranes and only 2% to the outer plasma membrane of the cell.

1.2 Evolution of Biomembranes

Membranes are quite old and thus have evolved over a long period of time. Indeed, membranes defined the boundaries of the first cells on earth and thus played a crucial role in the origin of life. The oldest microfossils that are viewed today as remnants of cells have an age of about 3.5×10^9 years. As a result of this long evolution, we now have an enormous variety of different cells and organelles, which live in very different environments. The interactions between the cells or organelles and their environments are mediated by their membranes. The basic function of these membranes is to act as

highly selective barriers for the exchange of molecules between the different spatial regions and compartments. In this way, they sustain concentration gradients between their two sides, which are used, for example, in order to produce energetic molecules or to propagate localized excitations along the membranes. Likewise, these membranes act as transducers for chemical, optical, or mechanical signals and as supporting surfaces for anchored polymers and polymer networks.

1.3 Universal Construction Principle

In order to fulfill its specific biological functions, each biomembrane is composed of a specific mixture of hundreds of different molecules. However, in spite of this complex chemical composition, all biomembranes exhibit the same universal construction principle: a *bilayer of lipid molecules,* which provides a two-dimensional solvent for the hydrophobic anchors of membrane proteins. Therefore, the simplest model systems for biomembranes are lipid bilayers without any proteins. When dissolved in water, these bilayers form closed bags or vesicles that resemble the closed compartments as formed by biomembranes.

1.4 Fluidity of Biomembranes

Under physiological conditions, biomembranes are in a fluid state; i.e., the membrane molecules can diffuse rapidly along these membranes. On the molecular scale, this fluidity is necessary for the proper functioning of membrane proteins. On the supramolecular scale, it ensures that the biomembrane is highly flexible and can undergo shape changes such as the formation of small spherelike buds. Therefore, both prokaryotic and eukaryotic cells adjust the lipid composition of their membranes in such a way that they remain in a fluid state irrespective of the ambient temperature and of other external conditions. Prokaryotic cells achieve this by increasing the number of unsaturated double bonds within the hydrocarbon chains of the lipid molecules. These unsaturated bonds act as defects within the bilayer that prevent the freezing of these membranes. Eukaryotic cells, on the other hand, increase the concentration of cholesterol within their membranes in order to maintain the fluidity.

2. MOLECULAR STRUCTURE OF LIPID BILAYERS

2.1 Lipid Molecules in Water

Lipids are amphiphilic molecules with a hydrophilic head group and usually two lipophilic (= hydrophobic) hydrocarbon chains. The head group of phospholipids and glycolipids contains a phosphate group and some sugar groups, respectively.

Those lipid molecules that are contained in biomembranes are essentially insoluble in water. More precisely, single lipid molecules can be dissolved in water only up to a critical monomer concentration X_*. This concentration is very small and decreases with increasing length of the hydrocarbon chains. For phospholipids with two identical chains containing $2N_c$ carbon atoms, one has $X_* \sim \exp(-1.7N_c)$ at room temperature, as can be measured for relatively small values of $N_c \lesssim 10$ (Cevc and Marsh, 1987). For the lecithin DPPC (dipalmitoyl phosphatidyl choline) with $N_c = 16$, this leads to the estimate $X_* \sim 10^{-12}$, i.e., less than one monomer per 10 μm^3 or per 10^{-8} mL of water.

2.2 Self-Assembly of Lipids

As soon as the lipid concentration in the aqueous solution exceeds the critical monomer concentration X_*, lipid molecules assemble into supramolecular structures. These structures are built up from *lipid bilayers* in which the polar head groups of the lipid molecules form the two lipid/water interfaces whereas the hydrophobic chains are buried within the bilayer and have essentially no contact with the aqueous solution. This process is an example of the so-called hydrophobic effect, which has a large entropic contribution arising from the configurational entropy of the hydrogen bond networks within the water (Tanford, 1991). Because of this effect, the lipid bilayers also arrange themselves in such a way that they have no edges and thus form closed vesicles or liposomes.

In practice, there are several preparation

methods in order to produce lipid vesicles starting with a lipid/water solution (see, e.g., Lasic, 1993). Small vesicles with a relatively narrow size distribution can be prepared from larger bilayer structures by sonification with ultrasound or by millipore extrusion. These vesicles are usually too small to be visible in the optical microscope. Relatively large vesicles with a linear size of the order of 10 μm are obtained if ordered stacks of membranes are swollen in a controlled way. In general, one then obtains a mixture of both unilamellar vesicles, consisting of a single bilayer, and multilamellar liposomes, consisting of several, closely packed bilayers.

In principle, the bilayers exchange lipid molecules with the aqueous solution surrounding them. However, since the monomer concentration X_* is so small, the exchange of molecules between the bilayers and the solution is extremely slow. As long as one considers phenomena that are fast compared to this rather slow exchange process, the chemical equilibrium that would arise from this exchange of molecules is blocked, and the number of lipid molecules within each bilayer is practically constant.

2.3 Lateral Diffusion and "Flip-flops"

Lipid bilayers are essentially two-dimensional systems: Their thickness is 4-5 nm, whereas their lateral extension often exceeds 10 μm. A two-dimensional system can exhibit distinct thermodynamic phases. Lipid monolayers at the water-air interface, for example, exhibit a large number of different phases, which have been studied by optical microscopy and x-ray and neutron scattering. Likewise, lipid bilayers always exhibit a fluid phase at high temperatures and one or several gel or solidlike phases at low temperatures. This article focuses on the *fluid states* of bilayers since these are the relevant states of biomembranes.

Within a fluid phase, the molecules can freely diffuse along the bilayer. The corresponding diffusion coefficients are typically of the order of 10^{-7}-10^{-8} cm^2/s. This implies that each lipid molecule covers of the order of 1 μm in 1 s.

While lateral diffusion within the fluid bilayer is rather rapid, "flip-flops," i.e., the transverse diffusion between the two monolayers, are much slower. In bilayers consisting of a single phospholipid, it takes usually several hours and more to exchange half of the phospholipid molecules between the two monolayers. In multicomponent bilayers, on the other hand, smaller molecules such as cholesterol can flip-flop more easily, and the corresponding time scale may be of the order of minutes.

2.4 Transport across Bilayers

Even though lipid bilayers are very thin, they provide selective barriers for the diffusive transport of molecules. Water and small uncharged molecules such as CO_2 or N_2 can permeate the bilayers: They first dissolve into their hydrophobic interior, cross it by simple diffusion, and finally dissolve into the aqueous solution on the other side of the membranes. The water permeability can be directly measured if one studies mixtures of H_2O with isotopically labeled water such as DHO or THO. On the other hand, lipid bilayers are essentially impermeable to ions and to larger uncharged molecules such as glucose. The transport of these latter molecules through biomembranes is facilitated by special membrane proteins such as ion channels and carriers. Some carriers represent ion pumps that provide an active, i.e., energy-consuming, transport mechanism against the concentration gradients (Darnell *et al.,* 1990; Alberts *et al.,* 1994).

3. ELASTIC PROPERTIES OF FLUID MEMBRANES

Fluid membranes have rather special elastic properties: Any shear deformation relaxes by flow within the membrane; i.e., the (zero-frequency) shear modulus of such a membrane vanishes. Thus, a fluid membrane exhibits only two types of elastic deformations: stretching and bending (Canham, 1970; Helfrich, 1973; Evans, 1974).

3.1 Stretching Deformations

The stretching of lipid bilayers is limited to rather small deformations, since they start to rupture as soon as their area is changed by about 1%. If a membrane segment with area $\mathcal{A}_0$ experiences the lateral tension Σ,

one has the area increase $\Delta\mathcal{A}$ with $\Sigma = K_{\mathcal{A}}\Delta\mathcal{A}/\mathcal{A}_0$. The area compressibility modulus $K_{\mathcal{A}}$ is of the order of $K_{\mathcal{A}} \simeq 200$ mJ/m^2, as has been measured in micropipette aspiration experiments; see Fig. 2. By this method, one can also determine the tension of rupture, Σ_{max}, which is of the order of a few mJ/m^2 (Evans and Needham, 1987).

3.2 Bending Deformations

Consider a planar membrane segment and let us focus on a cut perpendicular to such a membrane. If this membrane is bent, the surface of the cut is tilted; i.e., it is subject to a torque. This torque is proportional to the curvature of the membrane and to the length of the cut; the proportionality constant represents the *bending rigidity* κ, which has the dimension of an energy. For phospholipid bilayers, the bending rigidity is of the order of $\kappa \simeq 10^{-19}$ J $\simeq 20T$ as deduced from the thermally excited flickering of vesicles, see Sec. 6.1 (here and hereafter, the temperature T has energy units; i.e., T is a short-hand notation for Boltzmann constant $k_B \times$ temperature in kelvins).

As mentioned, the admixture of cholesterol to lipid bilayers increases their fluidity. At the same time, it also increases the bending rigidity of these membranes. For phospholipid bilayers, for example, the bending rigidity was measured to increase by a factor 3-4 if the bilayer contained 30% cholesterol. These combined effects of cholesterol are rather remarkable and must be the result of a long optimization process during evolution.

4. RELATED BUT DISTINCT SYSTEMS

4.1 Soap Films

The behavior of fluid membranes as discussed below is often counterintuitive. This is understandable since there is no macroscopic analog for such systems. The only fluid surfaces in our macroscopic world are soap films and soap bubbles. A soap film consists of a thin layer of water that is bounded by two monolayers of surfactant molecules. The latter molecules are also amphiphilic but they are soluble in water, at least to a certain extent: Their critical monomer concentration X_* typically varies between 10^5 and 10^7 molecules per 1 μm^3 or per 10^{-9} mL of water.

Each surfactant monolayer represents an air-water interface that is characterized by a relatively large interfacial tension. The latter tension represents the free energy per interfacial area and ensures that soap bubbles at-

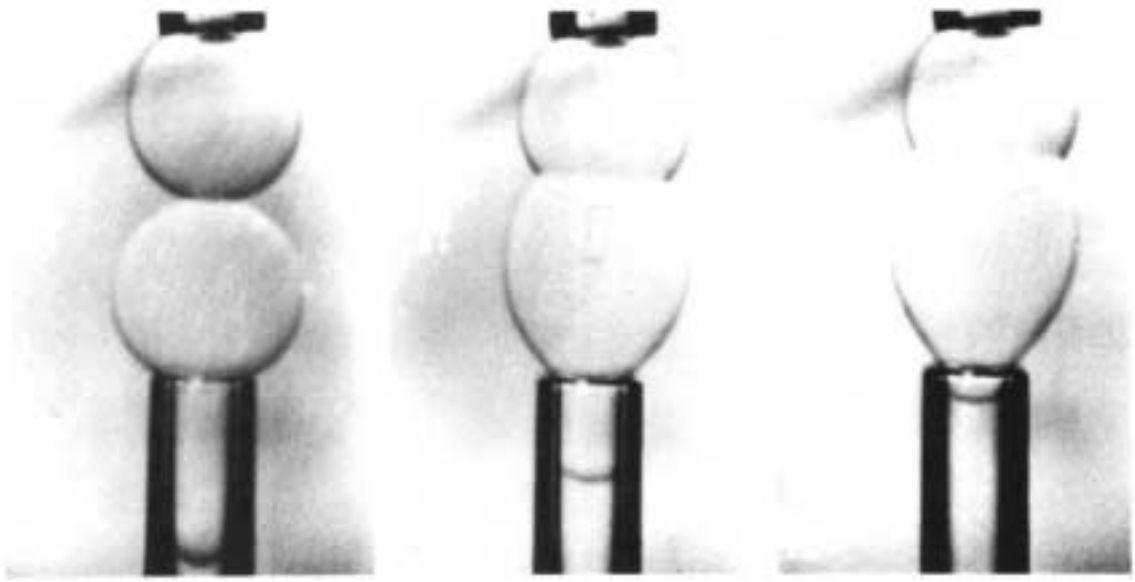

FIG. 2. Lipid vesicles may be sucked into small glass pipettes and can then be manipulated mechanically. The vesicle radii are about 10 μm. The top vesicle is almost spherical since it is exposed to a relatively large suction pressure. (Courtesy of E. Evans.)

tain a spherical shape. In addition, this interfacial tension is also responsible for the intrinsic instability of soap films: If one punches small holes into them, the tension acts to enlarge these holes and, thus, to rupture the soap films.

4.2 Surfactant Layers

Fluid monolayers of surfactant also form in multicomponent systems containing water and oil. Such mixtures exhibit many different phases in which these monolayers separate oil from water domains. Likewise, binary mixtures of water and surfactant may lead to liquid phases in which the surfactant molecules form bilayers separating two water domains. Since the critical monomer concentration X_* of the surfactant molecules is relatively large, these mixtures relax relatively fast toward states of thermal and chemical equilibrium, which are characterized by constant temperature and constant chemical potentials of the different components. These thermodynamic phases have been studied for a long time in physical chemistry and chemical engineering (for recent reviews, see Kahlweit and Lipowsky, 1996).

Surfactant layers are even more flexible than lipid bilayers, but they are also less stable and more sensitive to external perturbations. For example, it is usually not possible to transfer a single surfactant layer into a surfactant-free solution since this layer will dissolve rather rapidly. Likewise, it is hardly possible to manipulate surfactant layers by micropipettes or optical tweezers without destroying their structure. Therefore, in contrast to lipid bilayers, the behavior of *single* surfactant layers is not accessible to experimental studies.

4.3 Solidlike or Polymerized Membranes

Another class of membranes that has been recently studied in the theoretical physics community but will not be discussed in what follows consists of solidlike or polymerized membranes (for reviews, see Nelson *et al.,* 1989; Lipowsky, 1991). These latter membranes, which are characterized by a fixed connectivity of their building blocks, are more familiar since there are many examples for such membranes in our macroscopic world (such as an ordinary piece of paper, a thin film of rubber, or a fishnet). Solidlike membranes have a nonzero shear modulus, which leads to a coupling between bending and stretching deformations. Indeed, all bending deformations that change the Gaussian curvature of a solidlike membrane are necessarily coupled to strong stretching deformations of this membrane. Therefore, if the membrane (such as a piece of paper) is essentially unstretchable, it is impossible to deform it smoothly, i.e., without creating lots of folds or defects, from a planar into a spherical state. In contrast, such a shape transformation can be obtained easily for a fluid membrane; see Fig. 3.

5. THE MORPHOLOGY OF VESICLES

As mentioned, one can prepare relatively large vesicles with a linear size of the order of 10 μm that are bounded by a single bilayer. These vesicles can be directly observed in the optical microscope. One then finds that these vesicles exhibit a large variety of different shapes and various shape transformations as illustrated in Fig. 3.

A vesicle that is osmotically swollen experiences a lateral tension and, thus, attains a spherical shape just like a fluid droplet or a soap bubble. However, since water can permeate the membrane, the vesicle can adapt its volume and relax the tension. In this way, the membranes can attain an essentially tensionless state, the shape of which is governed by bending energies; compare Sec. 3 above. These shapes can be determined from systematic theories based on the relation between bending and curvature as described in the following section.

5.1 Shape of Homogeneous Membranes

First, consider a homogeneous fluid membrane with uniform elastic properties. As explained, the only elastic deformations that are relevant for fluid membranes are bending deformations governed by curvature.

5.1.1 Curvature and Bending Energy In general, each point of the membrane surface is characterized by its mean curvature

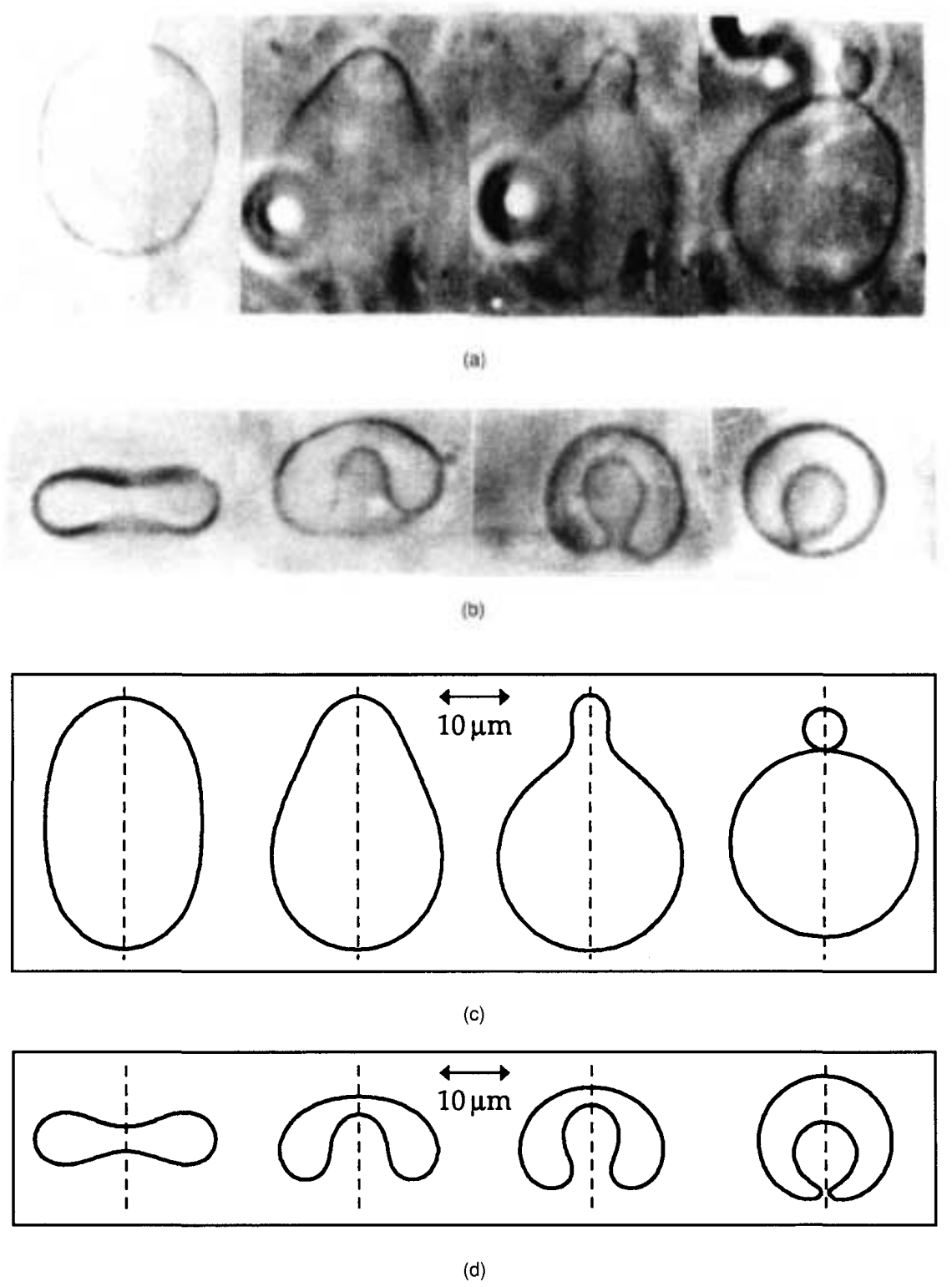

FIG. 3. Shape transformation of a single vesicle as observed via phase-contrast microscopy and calculated from curvature models. The transformations were induced by an increase in temperature that leads to an increase of the surface area of the vesicle. (a),(c) Budding, i.e., expulsion of a small vesicle from a larger one via the transformation from a prolate to a pear; (b),(d) inverse budding (or "endocystosis") via the transformation from a discocyte to a stomatocyte. The shapes are axisymmetric with respect to the broken line. In both cases, the bud is connected to the large vesicle by a small neck.

$$M \equiv (C_1 + C_2)/2 \tag{1}$$

and by its Gaussian curvature C_1C_2, where C_1 and C_2 are the two principal curvatures, which are equal to the inverse curvature radii.

If the two sides of the membrane are identical, the total bending energy has the form

$$\mathcal{H} = \oint d\mathcal{A}\, \tfrac{1}{2}\kappa(C_1 + C_2)^2 + \oint d\mathcal{A}\kappa_G C_1 C_2 \tag{2}$$

up to second order in the principal curvatures C_1 and C_2. The surface integrals extend over the whole membrane surface, and $d\mathcal{A}$ is the intrinsic area element. The two parameters κ and κ_G have the dimensions of energy and represent the bending rigidity and the modulus of the Gaussian curvature, respectively. For closed membranes without edges, the integral over the Gaussian curvature does *not* depend on the shape of the surface but only on its topology, as follows from the Gauss-Bonnet theorem.

The mean curvature term $\sim\oint d\mathcal{A}(C_1 + C_2)^2$ is a dimensionless and thus scale-invariant quantity. In fact, it is even invariant under arbitrary conformal transformations of three-dimensional space (Willmore, 1982).

5.1.2 Asymmetric Membranes In general, the two monolayers of the bilayer membrane may differ in their chemical composition, and the two sides of the bilayer may face different surroundings. This asymmetry can be described by a spontaneous mean curvature M_{sp} (Helfrich, 1973). Furthermore, the difference in density between the two monolayers adapts locally to the curvature: If the bilayer is bent, one of the monolayers is compressed and the other one is stretched (Evans, 1974).

The coupling between the density difference and the mean curvature leads to a constraint on the total mean curvature

$$\mathcal{M} \equiv \oint d\mathcal{A}M = \oint d\mathcal{A}\tfrac{1}{2}(C_1 + C_2), \tag{3}$$

which is proportional, for the *closed* bilayer, to the area difference of the two monolayers. This area difference can be changed by membrane proteins, which actively produce flip-flops of lipids between the two monolayers (Farge and Devaux, 1992). On the other hand, if flip-flops play no role, the total mean curvature would like to attain the preferred value, which corresponds to an unconstrained packing of the lipid molecules for which they all occupy the same (optimal) area (Miao *et al.,* 1994).

5.1.3 Constraints on Area and Volume In practice, vesicles exhibit a great variety of nonspherical shapes. This polymorphism arises, to a large extent, from two global constraints that are present for real vesicles:

1. The area of the bilayer membrane is constant (at constant temperature) since the exchange of molecules between the membrane and the solution can be neglected; and
2. the volume $\mathcal{V}$ of the vesicle does not adjust freely but is determined by the osmotic pressure P_{os} arising from those solutes that cannot permeate the bilayer; compare Sec. 2.4.

If X_{out} is the solute concentration outside of the vesicle and $\mathcal{N}_{in}$ is the number of solute molecules within the vesicle, one has $P_{os}\mathcal{V} \approx TX_{out}\mathcal{V} - T\mathcal{N}_{in}$ for small solute concentrations.

5.1.4 Shape Transformations and Limit Shapes As one changes a control parameter such as the osmotic pressure or the temperature, the shape of minimal bending energy usually evolves in a smooth way. However, for certain values of the control parameter, the shape undergoes a transformation that can be continuous or discontinuous. The shape transformations shown in Fig. 3 represent continuous transformations between a discocyte and a stomatocyte shape [Figs. 3(b) and 3(d)] and between a prolate and a pear shape at which the up-down symmetry of the shape is broken [Figs. 3(a) and 3(c)].

In addition, the shape may evolve into limit shapes in which different segments of the membrane surface start to come into contact. One type of limit shape consists of two segments connected by an infinitesimal neck that costs no bending energy; see the last shapes in Fig. 3.

5.1.5 Vesicles with Handles Recently, toroidal vesicles with one or several handles have also been studied both theoretically and

experimentally. For vesicles with two or more handles, the shape of minimal bending energy is degenerate even if one includes the various constraints on the vesicle shape (Jülicher *et al.,* 1993). In this degenerate region, theory predicts a diffusion process in shape space along a conformal mode with constant area, volume, and total mean curvature as shown in Fig. 4. Such a process has been recently observed by phase-contrast microscopy (Michalet and Bensimon, 1995).

5.2 Shape of Inhomogeneous Membranes

In general, a bilayer is composed of different types of molecules. In such a multicomponent system, the composition can become inhomogeneous, which affects the elastic properties and thus the shape of the membrane. Several cooperative phenomena that are driven by this coupling between composition and shape have to be distinguished. One rather general effect is provided by the budding of intramembrane domains.

5.2.1 Composition and Shape Small vesicles that are composed of two different lipids often exhibit a strong asymmetry in the composition of the two monolayers. This compositional asymmetry reduces the mismatch or "frustration" between the spontaneous curvatures of the two monolayers. Likewise, conelike molecules within the membrane tend to diffuse toward membrane regions with an appropriate curvature. Thus, curvature may induce phase segregation.

The phase diagram of a multicomponent bilayer usually exhibits one-phase regimes and two-phase coexistence regimes depending on the temperature and the membrane composition. When such a bilayer is prepared in the two-phase regime, it will undergo phase separation, which leads to the formation of lateral domains or patches within the membrane. These intramembrane domains often form ordered patterns as originally observed by freeze fracture and electron microscopy (Sackmann, 1990). The theoretical work on these domain patterns is reviewed in Lipowsky (1995b).

5.2.2 Domain-Induced Budding and Fission Now, let us focus on a single domain within the membrane. In general, this domain may have a spontaneous curvature that differs from the spontaneous curvature of the surrounding matrix. In addition, the edge of the intramembrane domain has an energy that is proportional to its length. Therefore, the domain has a tendency to attain a circular shape in order to minimize its edge energy.

However, a *flat* circular domain does not represent the state of lowest edge energy since the length of the edge can be further reduced if the domain forms a bud: The domain edge now forms the neck of the bud, and this neck narrows down during the budding process; see Fig. 5. Because of the edge energy, the domain must bud as soon as its linear size exceeds a certain critical size even if it has no spontaneous curvature. Simple theoretical estimates also show that the bud is likely to break off from the membrane matrix. There is some evidence for such budding and fission processes from experiments on vesicles that contain mixtures of phospholipids and cholesterol.

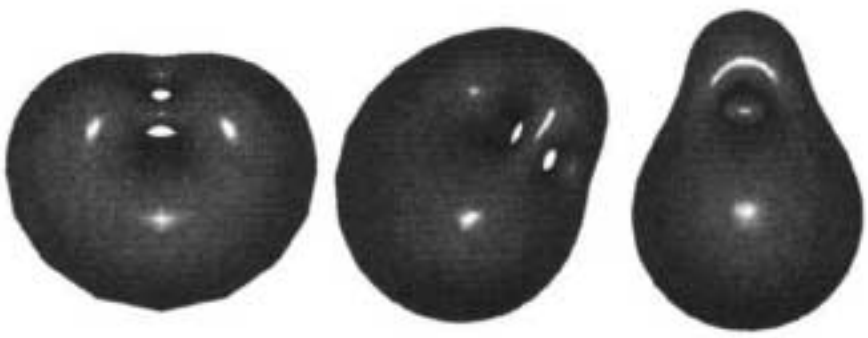

FIG. 4. Conformal diffusion of a vesicle with two handles: all three shapes have the same bending energy and the same area, volume, and total mean curvature.

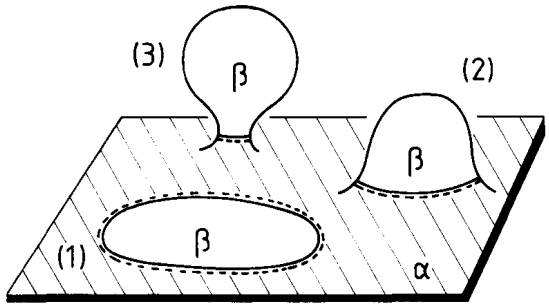

FIG. 5. Budding of the membrane domain β embedded in the membrane matrix α. The domain edge is indicated by the full-broken line. The length of this edge decreases during the budding process from (1) to (3).

5.2.3 Bud Size A vesicle that consists of two domains α and β could be obtained, for example, as a result of complete phase separation within the membrane. For such a vesicle, the shape of minimal bending energy exhibits a bud for a large range of parameters. This budded state attains a limit shape in which the bud β consists of a closed sphere that is connected to the mother vesicle α by an infinitesimal neck. The domain boundary with line tension σ is contained in this neck. The mean curvature M^β of this bud and the mean curvature M^α of the mother vesicle adjacent to this neck satisfy the general condition

$$\kappa^\alpha M^\alpha + \kappa^\beta M^\beta = \sigma/2 + \kappa^\alpha M^\alpha_{\rm sp} + \kappa^\beta M^\beta_{\rm sp}, \qquad (4)$$

where the bending rigidities κ^α and κ^β and the spontaneous curvatures $M^\alpha_{\rm sp}$ and $M^\beta_{\rm sp}$ of the α and β domains may be different (Jülicher and Lipowsky, 1996).

The size of the bud is given by $1/M^\beta$. If the spontaneous curvatures are negligible, the bud size becomes $1/M^\beta \approx 2\kappa^\beta/\sigma$ in the limit of a relatively small β domain. In this limit, the size of the bud is determined by the elastic properties of the domain alone, and domain-induced budding then represents a *local* mechanism.

5.2.4 Domain-Induced Budding of Biomembranes In biological cells, budding of intramembrane domains represents the first step in the production of vesicles for the intracellular transport between different cell compartments. These domains can grow by diffusion-limited aggregation of molecules within the membrane or by the adsorption of molecules from the surrounding medium.

The budding of these domains could be governed by their spontaneous curvature. The aggregated molecules may have membrane-spanning anchors that induce such a curvature in the bilayer. Likewise, the adsorption of coat proteins onto one side of the bilayer leads to an asymmetric membrane. In any case, the reduction of the edge energy of these domains during the budding process will always act to facilitate this process.

5.3 Adhesion of Vesicles

A vesicle that is attracted toward a surface gains adhesion energy but increases its bending energy. For large vesicles, the adhesion energy must dominate since it is proportional to the contact area whereas the bending energy is scale-invariant and thus independent of the vesicle size.

5.3.1 Contact Potential A vesicle near a wall or substrate experiences various molecular forces; see Sec. 7. The typical range of these forces is usually small compared to the size of the vesicle. In order to study the overall shape of the bound vesicle, the microscopic interaction can be replaced by a contact potential. This potential is described by a single parameter W, which is equal to the adhesion energy per unit area. The value of the potential strength W is determined by the competition between direct molecular forces and fluctuation-induced forces; see Sec. 7.

5.3.2 Adhesion Threshold Since the bound vesicle is curved more strongly than the free vesicle, the contact potential $|W|$ has to exceed a certain threshold

$$|W_a| = w_a\kappa/\mathcal{A} \qquad (5)$$

before the vesicle starts to adhere to the wall. The dimensionless coefficient w_a depends on the reduced volume $\mathcal{V}/\mathcal{A}^{3/2}$ and is of order 1 (Seifert and Lipowsky, 1995).

For an ensemble of vesicles with different sizes, the relation (5) implies that large vesicles with surface area $\mathcal{A} > w_a\kappa/|W|$ stick to the wall, whereas vesicles with smaller surface area do not. This difference in the size distribution of bound and free vesicles is accessible to reflectivity measurements.

6. SHAPE FLUCTUATIONS OF MEMBRANES

The membranes of vesicles undergo thermally excited shape fluctuations, which can be directly observed in the light microscope. For adhering vesicles, one can use reflection interference microscopy as shown in Fig. 6 (Rädler *et al.,* 1995). In this way, one can probe fluctuations with wavelengths between about 0.4 μm and the vesicle size. There are, however, many more length scales involved in these fluctuations, which have wavelengths down to molecular dimensions.

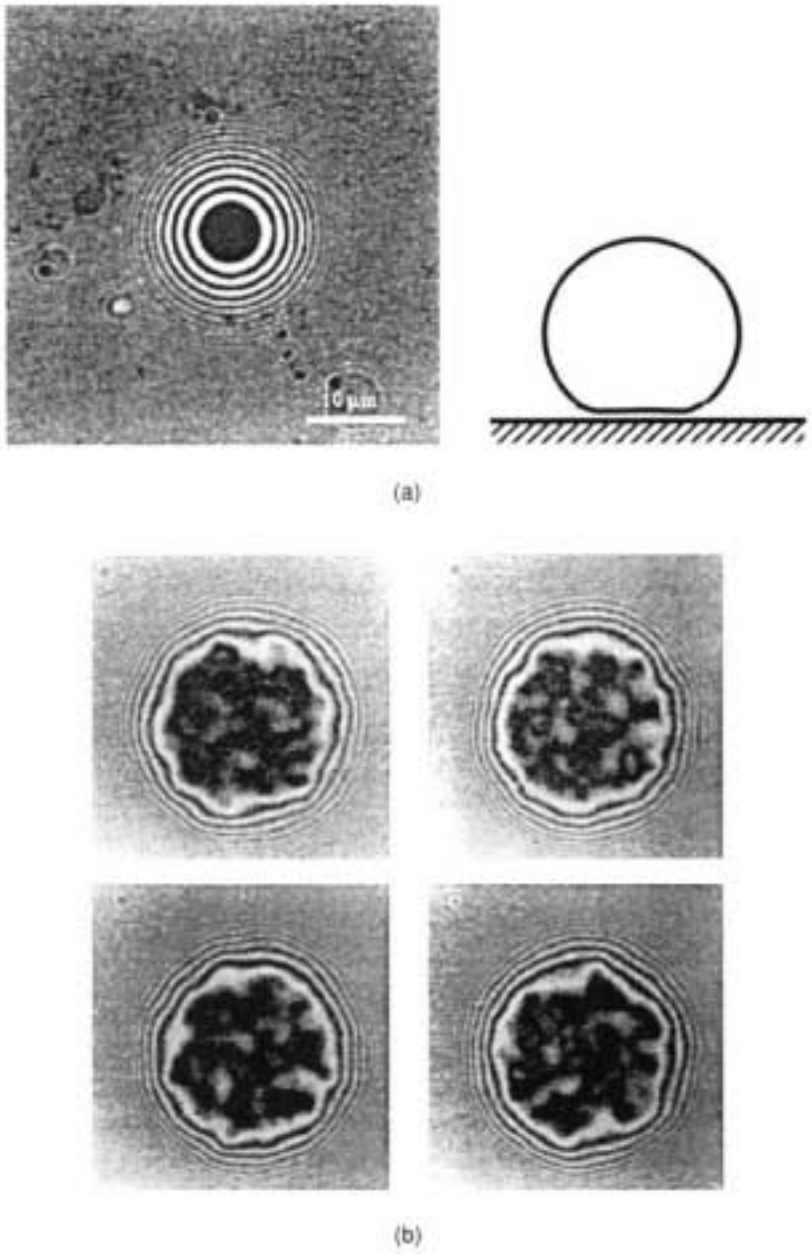

FIG. 6. Membrane of a bound vesicle as observed by reflection interference contrast microscopy. (a) Relatively large lateral tension, which suppresses all shape fluctuations, and (b) pronounced shape fluctuations for relatively small tension. (Courtesy of J. Rädler and E. Sackmann.)

6.1 Bending Modes or Undulations

On scales that are large compared to the membrane thickness, the typical shape fluctuations of fluid membranes are bending modes or undulations in which the surface area of the membrane remains unchanged.

6.1.1 Roughness Arising from Bending Modes An almost planar membrane segment that has bending rigidity κ and experiences the lateral tension Σ undergoes bending undulations that can be expanded in Fourier modes. The amplitude of these excitations depends on the temperature T. For a segment of linear size $L_\parallel$, these undulations lead to the membrane roughness $L_\perp$ with

$$\begin{aligned} L_\perp^2 &\approx (T/2\pi\Sigma)\ln(L_\parallel/\xi_\Sigma) \qquad \text{for } L_\parallel \gg \xi_\Sigma, \\ &\approx (T/16\kappa)L_\parallel^2 \qquad \text{for } L_\parallel \ll \xi_\Sigma, \end{aligned} \tag{6}$$

provided the crossover length $\xi_\Sigma \equiv (4\kappa/\Sigma)^{1/2}$ is large compared to the molecular scales (Brochard and Lennon, 1975). Thus, one has a rigidity-dominated regime for $L_\parallel \ll \xi_\Sigma$ and a tension-dominated regime for $L_\parallel \gg \xi_\Sigma$

6.1.2 Measurement of the Bending Rigidity Since the roughness $L_\perp \sim (T/\kappa)^{1/2}L_\parallel$ within the rigidity-dominated regime, measurements of this roughness can be used to determine the bending rigidity κ. In practice, this is done by optical microscopy of nearly spherical vesicles for which the undulations are expanded in spherical harmonics. In this way, one finds the typical values $\kappa \simeq (10 - 20)T$ for phospholipid bilayers (for a recent list, see Seifert and Lipowsky, 1995). It is, however, difficult to obtain high-precision values for κ. This is understandable since the bending rigidity of lipid bilayers is affected by small changes in their molecular structure arising, e.g., from conelike defects or from the molecular roughness of the lipid-water interfaces.

6.2 Thermal Fluctuations on Molecular Scales

The concept of a bending mode is no longer meaningful as soon as its wavelength becomes of the order of the membrane thickness. On these small scales, the molecular structure of the lipid-water interface should be taken into account. This interface is roughened by thermal fluctuations, as has been observed in computer simulations (Pastor, 1994) and has been deduced from scattering experiments (König *et al.,* 1992; Wiener and White, 1992; McIntosh and Simon, 1993). These thermal fluctuations correspond to relative displacements or deformations of the lipid head groups: Since they will, in general, change the surface area of the lipid-water interface, they are governed by an effective tension Σ_{eff}. The roughness arising from these fluctuations is set by the length scale $(T/2\pi\Sigma_{\text{eff}})^{1/2}$, which is expected to be of the order of a few angstroms.

6.3 Persistence Length on Large Scales

On sufficiently large scales, a fluid surface that does not experience any lateral tension starts to crumple, i.e., to behave as a random surface without any average orientation. This happens as soon as its size exceeds the so-called persistence length (de Gennes and Taupin, 1982; Gompper and Kroll, 1995). For phospholipid bilayers with bending rigidities $\kappa \gtrsim 10T$, the persistence length is, however, very large compared to the largest accessible sizes of these bilayers. Therefore, under normal circumstances, lipid bilayers (and biomembranes) do not behave as random surfaces with no average orientation.

7. GENERIC INTERACTIONS OF TWO MEMBRANES

The behavior of interacting membranes is governed by the interplay of direct interactions arising from the forces between the molecules and shape fluctuations such as bending undulations that act to renormalize these interactions.

7.1 Direct Interactions between Rigid Membranes

The direct interaction $V(l)$ between two rigid membranes at separation l can be measured by the surface force apparatus consisting of two mica surfaces onto which the membranes are immobilized (Marra and Israelachvili, 1985). The simplest example is provided by lipid bilayers that

1. are electrically neutral and
2. interact across a water layer that contains no macromolecules or colloids.

In this case, the interaction potential $V(l)$ is composed of a repulsive hydration and an attractive van der Waals interaction and has the schematic form shown in Fig. 7(a).

Lipid bilayers may become charged by adsorption of ions from the solution or by dissociation of their head groups. They then exhibit electric double layers, which usually lead to *repulsive* interactions between the surfaces as predicted by the classical Poisson-Boltzmann theory. The combination of van der Waals and electrostatic interactions often leads to a potential barrier as shown in Fig. 7(b).

7.2 Renormalization by Bending Undulations

Two interacting membranes that are in thermal equilibrium with the surrounding liquid undergo bending undulations. Since the configurational entropy of the undulations increases with the membrane separation, these fluctuations lead to a repulsive force that drives the membranes apart and, thus, reduces the attractive part of their interaction. It will be tacitly assumed here that the interaction potential $V(l)$ is effectively short-ranged and decays faster than $\sim 1/l^2$ for large l. Van der Waals forces eventually decay as $\sim 1/l^4$ and thus belong to this strong-fluctuation regime.

7.2.1 Repulsive Interactions If the interaction $V(l)$ between the membranes is effectively repulsive, the membranes can be kept together by an osmotic pressure P arising, e.g., from macromolecules in the surrounding solution that cannot permeate the membranes. In this case, the membranes are bound for finite $P > 0$ but unbind in the limit of zero P. The mean separation $\langle l \rangle$ behaves as $\langle l \rangle \sim 1/P^{\psi}$ for small P with the unbinding exponent $\psi = \frac{1}{3}$. As the membranes unbind, the probability $\mathcal{P}_2$ for pair contacts or two-membrane collisions decays to zero as $\mathcal{P}_2 \sim 1/\langle l \rangle^{\zeta_2}$ with the contact exponent $\zeta_2 = 3$. This is completely analogous to the behavior of one-dimensional strings, which are governed by a finite line tension.

The behavior of the mean separation $\langle l \rangle$ can be obtained from the entropic or fluctuation-induced interaction $V_{\text{fl}}(l) \sim 1/l^2$, as deduced by Helfrich (1978) using a heuristic scaling picture even though this picture implies the incorrect behavior $\mathcal{P}_2 \sim 1/\langle l \rangle^2$ for the contact probability.

7.2.2 Attractive Interactions and Continuous Unbinding For a direct interaction as shown in Fig. 7(a) that is dominated by attractive van der Waals forces, the membranes undergo a *continuous* unbinding transition from a bound state at low temperatures to an unbound state at high temperatures, as was first predicted theoretically (Lipowsky and Leibler, 1986). If the interaction potential $V(l)$ is parametrized by the effective potential depth $|U|$ and the effective potential range l_v, the unbinding temperature is given by

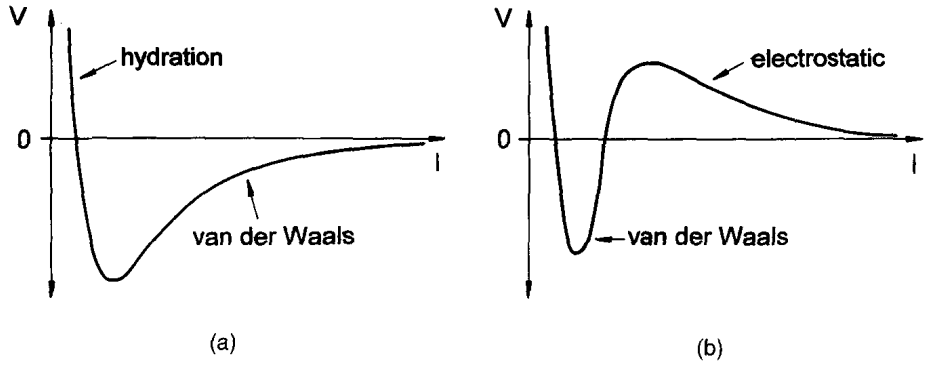

FIG. 7. Direct interaction V between two planar membranes as a function of the membrane separation l: (a) hydration and van der Waals interaction between electrically neutral membranes; (b) hydration, van der Waals and electrostatic interaction between electrically charged membranes leading to a potential barrier.

$$T_u \simeq \sqrt{\kappa |U| l_v^2}. \quad (7)$$

As one approaches $T = T_u$ from below, the mean separation $\langle l \rangle$ of the membranes diverges as $\langle l \rangle \sim 1/|T - T_u|$, and the strength $|W|$ of the renormalized potential vanishes as $|W| \sim -|T - T_u|^2$. The same critical behavior is found for two interacting strings in two dimensions where the unbinding process represents a wetting transition.

The adhesion of large vesicles is also diminished by thermally excited fluctuations; compare Fig. 6. From the relation (5) and the behavior $|W| \sim -|T - T_u|^2$ of the adhesive strength, one obtains the unbinding temperature $T_u^{\text{ves}} \approx T_u - c\kappa l_v/\sqrt{\mathcal{A}}$ for large vesicles with surface area $\mathcal{A} \gg \kappa/|U|$

7.2.3 Potential Barriers and Discontinuous Unbinding The direct interaction $V(l)$ may exhibit a potential barrier as shown in Fig. 7(b). In this case, the unbinding transition can be continuous or discontinuous depending on the relative strength of the potential barrier. If the potential barrier is relatively weak, the undulations "tunnel" through the barrier and the unbinding transition is continuous. This is again analogous to one-dimensional strings in two dimensions, which tunnel, however, through *any* potential barrier that decays faster than $1/l^2$ for large l. In contrast, two-dimensional membranes cannot tunnel through sufficiently strong barriers. In the latter situation, they are trapped by the barrier, and the unbinding transition is discontinuous.

7.3 Tension-Induced Adhesion

A lateral tension Σ acts to suppress the bending undulations and thus to decrease the fluctuation-induced repulsion. In fact, this interaction now becomes short-ranged and decays exponentially as $V_{\text{fl}}(l) \sim \exp(-l/l_\Sigma)$ for separations $l \gg l_\Sigma \equiv (T/2\pi\Sigma)^{1/2}$. Thus, for sufficiently large separations, this fluctuation-induced repulsion cannot compete with the attraction arising from van der Waals forces, and the membranes form a bound state in the presence of lateral tension. In the limit of vanishing tension, the membranes unbind provided the temperature exceeds the unbinding temperature T_u.

It has been argued by Helfrich (1989) that some lipid bilayers show a more complex behavior in the low-tension regime and that these layers develop a superstructure that acts as an additional reservoir for membrane area. This issue remains to be clarified.

7.4 Repulsive Interactions at Small Separations

It has been well established by many experiments that lipid bilayers in aqueous solution experience a strong repulsion at small separations of the order of 1 nm (Rand and Parsegian, 1989). The corresponding force per unit area or disjoining pressure, P, is observed to decay exponentially as $P \sim \exp(-l/l_{\text{eff}})$, where the effective decay length l_{eff} is of the order of a few angstroms; see Fig. 8. It was originally thought that this short-ranged repulsion represents a hydration effect and reflects the perturbed water structure in front of the polar head group (Marcelja and Radic, 1976). On the other hand, a similar repulsive force can also arise from the molecular roughness of the lipid-water interfaces (Israelachvili and Wennerström, 1990). In general, both mechanisms should contribute, and their relative importance will depend on the temperature and on the lipid-solvent composition (Lipowsky and Grotehans, 1994).

8. BUNCHES AND STACKS OF MEMBRANES

Lipid bilayers in solution often form bunches in which several membranes are, on average, parallel to each other. Two different geometries must be distinguished:

1. free bunches in solution, as shown in Fig. 9(a), and
2. bunches that adhere to a rigid surface or wall; see Fig. 9(b).

The latter geometry is obtained, e.g., by spreading a concentrated lipid solution on a glass slide.

The structure of such a bunch can be characterized by its density profile, which depends on the mean separations of the membranes within the bunch. If the shape fluctuations of these membranes are strong, they drive the membranes apart and lead to loosely bound or highly swollen states (Lipowsky, 1995a).

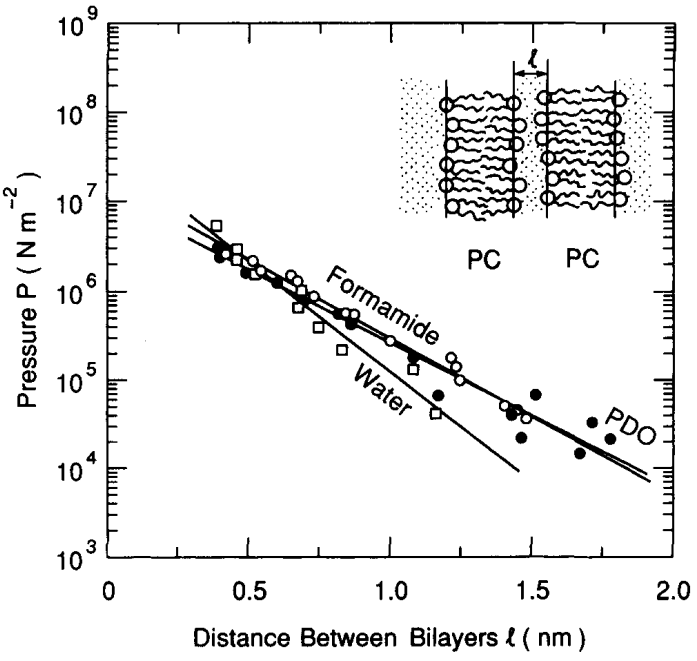

FIG. 8. Disjoining pressure P of phosphatidyl choline (PC) bilayers as a function of the mean separation $\langle l \rangle$ of lecithin or PC bilayers for the three solvents water, formamide, and 1,3-propanediol (PDO) (McIntosh *et al.,* 1989).

8.1 Free Membranes in Solution

For a free bunch of N identical membranes as shown in Fig. 9(a), all membranes have the same bending rigidity κ, and each adjacent pair of membranes interacts with the direct interaction $V(l)$. If the bunch is kept together by short-ranged attractive interactions arising, e.g., from van der Waals forces, it undergoes a *unique* unbinding transition as observed

1. in experiments for up to 20 sugarlipid membranes (Mutz and Helfrich, 1989) (see Fig. 10), and
2. in Monte Carlo simulations for up to four membranes (Netz and Lipowsky, 1993).

The unbinding temperature T_u^f of the free bunch is *independent* of N and thus identical to the unbinding temperature of two membranes.

Analytical work on bundles of strings (Hiergeist *et al.,* 1994) leads to the prediction that the mean separation $\langle l \rangle_n$ of the adjacent

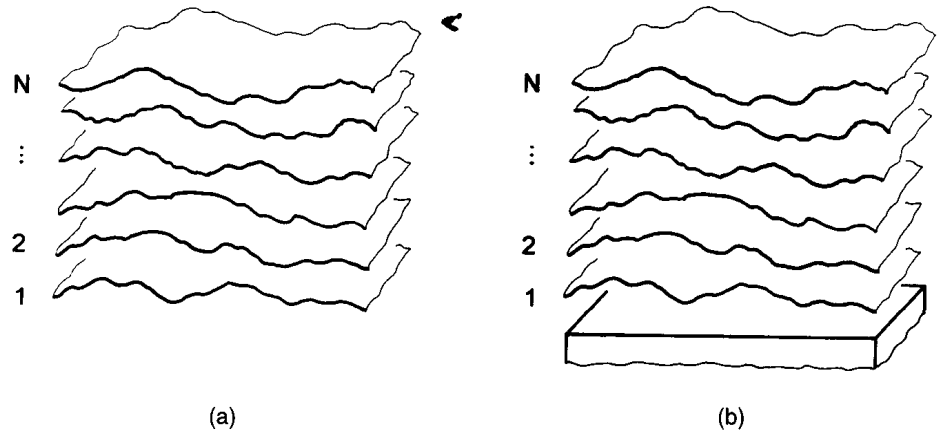

FIG. 9. Bunches of N fluctuating membranes: (a) Free bunch in solution; (b) bunch adhering to a rigid surface or wall.

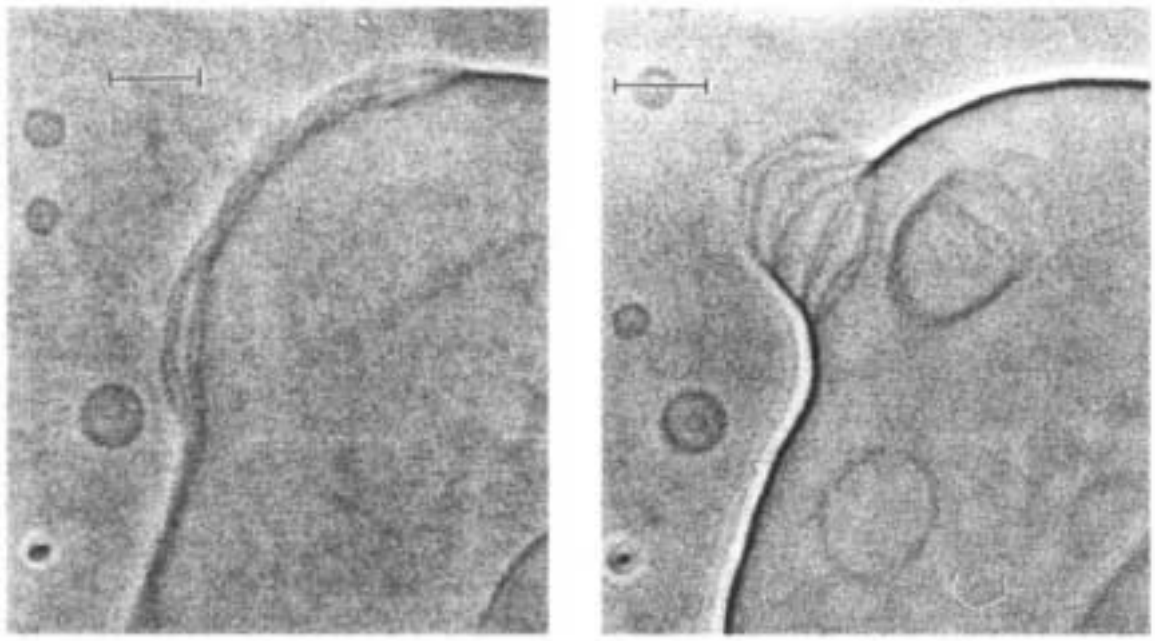

FIG. 10. Unbinding or adhesion transition as experimentally observed for a bunch of eight lipid bilayers in aqueous solution. (Left) For $T \simeq 22.4$ °C, the membranes undulate very strongly and then appear as thick fuzzy lines. (Right) For $T \simeq 22.1$ °C, the membranes form a bound state that corresponds to the sharp dark line. The water between the membranes has been squeezed into the large water pocket. The bars represent 10 μm. (Courtesy of W. Helfrich.)

membranes labeled by n and $n + 1$ is given by

$$\langle l \rangle_n \sim 1/n(N - n)|T - T_u^f|^\psi \qquad \text{with } \psi = 1. \tag{8}$$

Thus, all length scales should diverge with the universal unbinding exponent $\psi = 1$ but should exhibit an amplitude that depends strongly on N and on the position n within the bunch. This implies that the temperature interval in which the behavior is dominated by fluctuations shrinks as $\sim 1/N$ for large N. Therefore, for large N the continuous unbinding transition will appear to be discontinuous.

8.2 Membranes at a Rigid Surface

In the case of N membranes attracted toward a rigid surface or wall, as shown in Fig. 9(b), the unbinding behavior depends on the relative strength of the surface-membrane and the membrane-membrane attraction. There are essentially two possibilities:

1. If the attraction toward the substrate is sufficiently weak, one has a sequence of two transitions: the whole N-bunch unbinds from the substrate at the unbinding temperature $T = T_u^b < T_u^f$ and then undergoes the transition toward completely unbound membranes at $T = T_u^f$
2. If the attraction toward the rigid surface is relatively strong, one has a sequence of N unbinding transitions and thus a sequence of unbinding temperatures T_u^n with $T_u^f < T_u^n \leq T_u^1$. At each of these transitions, a single membrane peels off from the bunch. Such peeling processes should always occur during the formation of vesicles from oriented samples. Thus, in this case, the presence of the rigid surface is still felt by the outermost membrane even in the presence of many intervening membranes.

8.3 Limit of Lyotropic Liquid Crystal

In the limit of large N, the membrane stack becomes a lyotropic liquid crystal, which can be studied by x-ray and neutron scattering.

8.3.1 Power-Law Peaks of the Scattering Intensity The renormalization of the direct interaction $V(l)$ by bending modes

with small wavelengths leads to the effective potential $V_{\text{eff}}(l)$, which determines the mean separation $\langle l \rangle$ via $\partial V_{\text{eff}}(l)/\partial l = 0$. Expanding this effective potential up to second order in the displacements, one obtains a harmonic model, which leads to the prediction that the scattering intensity $S(q)$ exhibits the power-law behavior

$$S(q) \sim (q_z - q_m)^{-(2-X_m)} \quad \text{with } X_m \equiv Tq_m^2/8\pi\sqrt{\kappa \nu_{\text{eff}}} \tag{9}$$

in reciprocal space along the q_z direction close to $q_z = q_m = 2\pi m/\langle l \rangle$ with $m = 1$ 2, . . . and $\nu_{\text{eff}} \equiv \partial^2 V_{\text{eff}}(l)/\partial l^2$ at $l = \langle l \rangle$. These power-law peaks are known as Landau-Peierls singularities and have been studied by x-ray scattering on lamellar phases of oil-water-surfactant mixtures (Meunier *et al.,* 1987).

8.3.2 Melting of Lamellar States Lamellar phases of oil-water-surfactant mixtures often melt into isotropic phases. If the melting is initiated by bending undulations, one may assume that the lamellar phase becomes unstable as soon as the roughness $\xi_\perp$ of the membrane separation satisfies $\xi_\perp > c_* \langle l \rangle$ (de Gennes and Taupin, 1982) (note that the roughness of a single "tracer" membrane within the liquid crystal increases logarithmically with the size of the membrane). This relation corresponds to the so-called Lindemann criterion for the melting of solids. Within the harmonic model, this implies that the lamellar phase becomes unstable as soon as the bending rigidity becomes too small and satisfies $\kappa < T^2/(2\pi c_*)^2 \nu_{\text{eff}} \langle l \rangle^4$.

9. POLYMER-DECORATED MEMBRANES

In addition to the lipid bilayer, biomembranes contain a complex mixture of macromolecules. These molecules, which are anchored in the membranes, are usually connected to a network of relatively stiff, rodlike filaments that belong to the so-called cytoskeleton within the cell. Likewise, the outer plasma membrane is often covered by a "coat" of polysaccharides, i.e., of branched polymers, which are also anchored within the membranes. These systems can be modeled, to a certain extent, by the decoration of lipid bilayers with polymers.

9.1 Anchored Polymers

Any polymer with one or several hydrophobic segments that fit into the hydrophobic interior of the lipid bilayer can be anchored to this bilayer. The simplest geometry is obtained for a polymer with a single anchor attached to one of its ends. Artificial systems of this kind are water-soluble polymers covalently bound to a single lipid molecule (Lasic, 1994) or block copolymers with a short hydrophobic block. Another possibility is to use polymers with hydrophobic side groups (Simon *et al.,* 1995). In this case, the polymers can be attached by several anchors. Such a system is shown in Fig. 11. In contrast to polymers grafted to solid surfaces, these anchored polymers can diffuse laterally along the fluid membrane.

If the nonanchored segments of the polymer are effectively repelled from or attracted to the membrane surface, the anchored polymer is in a desorbed or in an adsorbed state, respectively. In the desorbed state, a polymer that is attached to the membrane by a single anchor has the form of a "mushroom," the size of which is comparable to the dissolved polymer. Weak adsorption leads to squashed mushrooms; strong adsorption, to polymer "pancakes" that are tightly bound onto the membrane surface.

9.2 Dilute and Semidilute Regimes

First, consider effectively repulsive interactions between the anchored polymer and the membrane surface. If the concentration of anchors within the membrane is sufficiently small, the anchored polymers form well-separated mushrooms. This dilute regime applies up to the overlap concentration at which the membrane surface becomes completely covered by anchored polymers. If one increases the coverage beyond this overlap value, the polymers start to squeeze and to stretch each other and one enters the brush regime. This brush regime extends up to a maximal coverage at which the loss of entropy arising from the stretched state of the polymers exceeds their anchoring energy.

A similar distinction applies to anchored

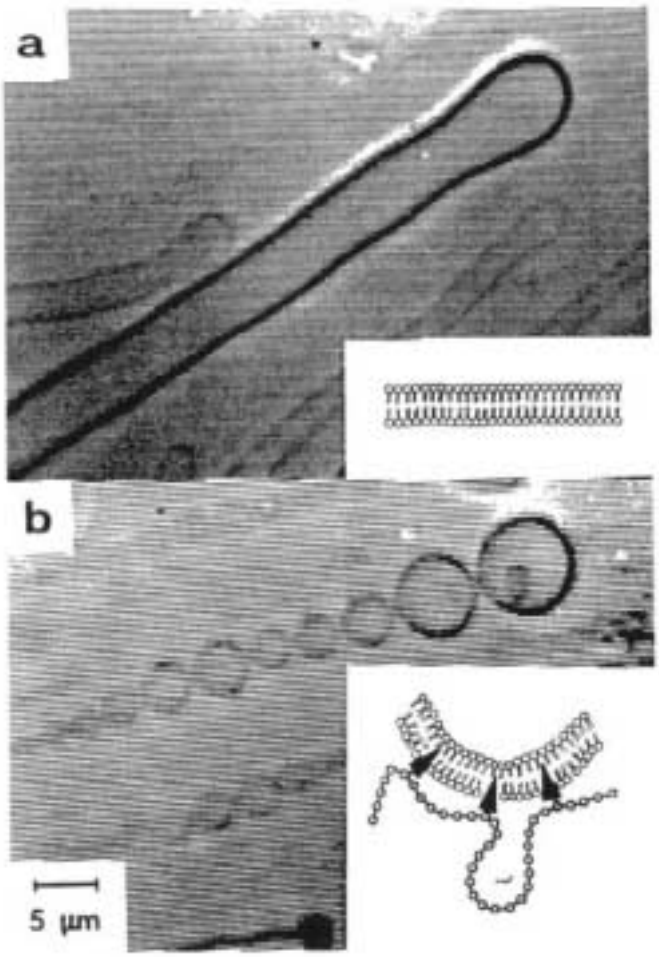

FIG. 11. Shape transformation of (a) a tubular vesicle into (b) a string of spheres as induced by the addition of polymers with hydrophobic side groups. This transformation is presumably governed by the interaction of these side groups with the lipid bilayer. (Courtesy of H. Ringsdorf.)

polymers that are adsorbed onto the membrane. In the dilute regime, one has well-separated pancakes. Beyond the overlap concentration, these pancakes start to interpenetrate each other and to form a semidilute adsorption layer.

9.3 Polymer-Induced Curvature

A bound polymer or mushroom suffers a loss of entropy compared to the free state. This entropy loss depends on the shape of the membrane; see Fig. 12. Therefore, the mushroom exerts entropic forces on the membrane that bend the membrane away from the polymer (Lipowsky, 1995b).

In the unbound state, a linear flexible polymer consisting of N monomers of linear size a forms a coil of linear dimension $R_{po} \simeq aN^{\nu}$ with $\nu \simeq 3/5$ for good solvents. In the bound mushroom state, the polymer induces the "spontaneous" mean curvature

$$M_{\rm sp} \sim T/\kappa R_{po} \sim T/\kappa a N^{\nu} \tag{10}$$

of the decorated membrane. In a similar way, curvature is induced by a polymer brush that is attached to the membrane in a nonsymmetric way. If the polymer is adsorbed onto the membrane, on the other hand, it induces the opposite sign of the curvature: The membrane now bends toward the membrane in order to maximize the number of contacts.

9.4 Polymer-Induced Adhesion

The adhesion of cell membranes is mediated by rodlike polymers that have a linear extension of 10-30 nm. In the absence of these sticky rods, the cell membranes experience an effectively repulsive interaction arising from the electric charges on their surfaces. The adhesive strength mediated by

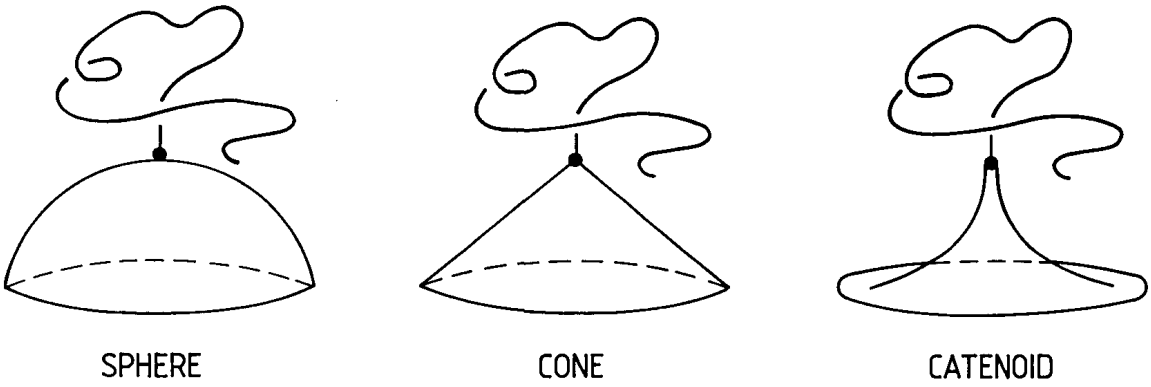

FIG. 12. A polymer attached to the membrane by a single anchor forms a mushroom that bends the membrane by entropic forces. For the three shapes of the membrane segment shown here, the cone leads to the highest entropy for the anchored polymer.

the sticky rods depends on the concentration X of their anchors within the membrane.

Since this strength must exceed a certain threshold value in order to overcome the repulsion arising from the membrane undulations, the anchor concentration must also exceed a critical value X_c. If the rod anchors attract one another, the bilayers may undergo phase separation into polymer-rich domains with $X > X_c$ and polymer-depleted domains with $X < X_c$. In the latter case, the membranes will only adhere via the polymer-rich domains.

10. APPLIED ELECTROMAGNETIC FIELDS

For the phenomena discussed in the previous sections, the molecular structure of the lipid bilayer is not perturbed in an essential way. In contrast, the application of pulsed electric fields or of optical tweezers built up from a laser beam strongly perturbs the bilayer structure, which leads to new cooperative effects.

10.1 Alternating Electric Fields

The lipid membrane has a dielectric constant (or permittivity) $\epsilon_M \simeq 2$, which is small compared to the dielectric constant $\epsilon_W \simeq 80$ of water. Likewise, the electrical conductivity γ_W of water is large compared to the conductivity γ_M of the lipids. This implies that the electric field is *amplified* within the membrane. This is the basic mechanism that is responsible for the electroporation and electrofusion of lipid bilayers and biomembranes (Neumann *et al.*, 1989; Chassy *et al.*, 1992).

If the alternating electric field $\mathbf{E}_W \exp[i\omega t]$ is applied in the water and the two lipid-water interfaces are treated as dividing surfaces with no intrinsic width, the transmembrane potential $\Delta\Phi_M$ across a planar membrane is given by

$$\Delta\Phi_M = E_M a_\perp$$
$$\text{with } E_M = \left[\frac{(\omega\epsilon_W)^2 + \gamma_W^2}{(\omega\epsilon_M)^2 + \gamma_M^2}\right]^{1/2} E_W, \qquad (11)$$

where $a_\perp$ represents the thickness of the membrane (this relation follows from Maxwell's equations and the continuity equation for the charge carriers). For water without salt, the square root prefactor is about 5×10^3.

10.2 Electroporation

If the lipid membrane is exposed to a transmembrane potential $\Delta\Phi_M$ that exceeds $\simeq 0.2$ V for an extended period of time, the membrane ruptures in an irreversible way. On the other hand, if one applies a potential $\Delta\Phi_M$ of the order of 1 V for a relatively short time period Δt within the range 10^{-7} s $\leq \Delta t \leq 10^{-4}$ s, one obtains a reversible electrical breakdown of the lipid bilayer: The permeability of the bilayer is strongly increased right after the pulse has been applied but then relaxes back to its original value. This behavior is observed both for artificial lipid bilayers and for biomembranes. In both

cases, the high-permeability state arises from the formation of pores within the lipid membrane. These pores have been directly observed by freeze-fracture electron microscopy.

10.3 Electrofusion

Two membranes that are in close contact can be fused by applying a short electrical pulse. It is widely believed that this process of electrofusion is induced by the simultaneous electroporation of both membranes within the contact area. It has also been found, however, that fusion can even occur when the membranes are treated with electrical pulses before being brought into close contact. Electrofusion is a universal fusion mechanism that has been applied to many different types of biomembranes. An example in shown in Fig. 13.

The initial fusion step presumably consists in the juxtaposition of two pores in the two adjacent membranes. The next step should be the formation of a neck or "wormhole" that bridges the gap between the two membranes. Several intermediate structures that could be involved in this topological transformation have been proposed.

10.4 Optical Tweezers

Optical tweezers, arising from a laser beam that is focused through a microscope objective, provide localized light traps and can be used to manipulate various objects in the micron range. Recently, such tweezers have been directly applied to lipid bilayers and were found to induce novel shape transformations. When applied to cylindrical vesicles consisting of a single bilayer, the tweezers induce a pearling instability, which spreads from the trap and eventually produces a chain of pearls that again resembles the Plateau-Rayleigh instability of capillary tubes. When applied to bunches of several bilayers, the light trap acts to unbind the membranes locally and to induce a characteristic shape of the loosely bound structure (Bar-Ziv *et al.,* 1995).

It is presently believed that the focused laser beam destroys the bilayer structure locally and acts to pull lipid molecules into the light trap. This process should generate a lateral tension for the rest of the membrane, which is not exposed to the beam. A theoretical model has been developed that is based on this interpretation and has been used to calculate the selected wavelength of the pearling instability (Goldstein et al., 1996).

11. OUTLOOK ON APPLICATIONS

The tendency of lipids to form closed compartments such as vesicles is used in pharmacology, food industry, and cosmetics in order to enclose and transport drugs, enzymes, vitamins, moisturizers, and other in-

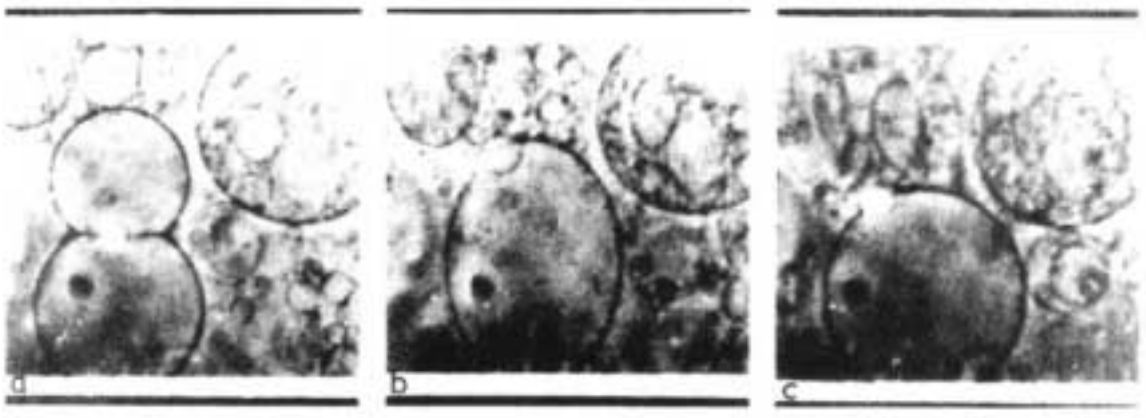

FIG. 13. Electrofusion of two lipid vesicles as observed by phase contrast microscopy: (a) The two vesicles, with diameters of about 45 and 37 μm, are brought into close contact by an alternating electric field; (b) fused vesicle about 1 s after the application of a short electrical pulse; (c) the fused vesicle, which has a diameter of about 51 μm, becomes roughly spherical when the alternating field is switched off. (Courtesy of U. Zimmermann.)

gredients. The delivery of drugs via vesicles can be improved by the decoration with polymers that are attached to the lipid head groups and that prevent the uptake of these vesicles by lymphocytes in the blood. Furthermore, vesicles composed of lipid mixtures might be used in order to transport drugs directly through the skin and, thus, to replace the use of hypodermic needles.

Other interesting areas are attempts to attach lipid layers to solid substrates in order to build up new types of biosensors, or to cover artificial bones by such layers in order to improve their biocompatibility.

The mechanisms of electroporation and electrofusion have been applied to many areas of biotechnology. For example, electroporation is now widely used in order to transfer genes into all kinds of cells.

In summary, flexible membranes already play an important role in various soft-matter technologies. It seems rather likely that an improved understanding of the physics of these systems will lead to new technological applications: The future is in the flexible!

GLOSSARY

Aggregation Colloids: Supramolecular structures that arise from the self-assembly of single molecules or monomers in solution.

Amphiphilic Molecules: Molecules that have a lyophilic part, which dissolves in the solvent, and a lyophobic part, which is insoluble in the solvent. One important example is molecules dissolved in water that have a polar hydrophilic part and a nonpolar hydrophobic part.

Anchored Polymer: Polymer chain attached to the bilayer membrane by one or several hydrophobic segments that fit into the hydrophobic interior of the bilayer. If the nonanchored segments of the polymer are effectively repelled or attracted to the membrane surface, the anchored polymer attains the form of a "mushroom" or "pancake," respectively.

Area Compressibility Modulus: Elastic modulus of membranes that governs their resistance against stretching.

Bending Rigidity: Elastic modulus of membranes that governs their resistance against bending.

Bilayer: Membrane consisting of two monolayers that are arranged in such a way that the polar head groups of the lipid molecules form the two lipid-water interfaces, whereas the hydrophobic chains are buried within the bilayer and have essentially no contact with the aqueous solution. The thickness of these bilayers is 4-5 nm.

Budding: Shape transformation in which the membrane produces a small bud that is essentially spherical and connected to the original membrane via a small neck.

Conformal Diffusion: For vesicles with two or more handles, the shape of the vesicle can undergo a diffusion process along degenerate states that are related by conformal transformations.

Critical Monomer Concentration: This concentration represents

1. the upper limit for the concentration of amphiphilic monomers in solution and
2. the critical concentration at which the amphiphilic molecules start to aggregate into supramolecular structures.

It is also called critical micelle concentration since many surfactant molecules assemble into micelles.

Curvature: Any point on a two-dimensional surface that is embedded in three-dimensional space can be characterized by two principal curvatures, C_1 and C_2, which are equal to the inverse curvature radii. The mean curvature is given by $M \equiv (C_1 + C_2)/2$

Decorated Membrane: Lipid bilayer with anchored polymers. For fluid bilayers, these polymers can diffuse along the membrane surface.

Direct Interaction: Interaction between two rigid membranes arising from the forces between the molecules. This interaction can be measured by the surface-force apparatus in which the membranes are immobilized onto two mica surfaces.

Electrofusion: Two adjacent membranes that are separated by a small water layer can be fused by the application of an electrical pulse, which is believed to induce pores through both membranes.

Electroporation: Pores that go through a bilayer can be induced by the application of a short electrical pulse with a voltage of the order of 1 V.

Flip-flops: The slow exchange of molecules between the two monolayers of a bilayer membrane.

Fluid Membranes: Membranes for which shear deformations relax by flow within the membrane. The molecules within such membranes undergo rapid lateral diffusion.

Hydrophobic Effect: The tendency of amphiphilic molecules in water to form supramolecular structures in which the hydrophilic groups of these molecules form the outside interface toward the aqueous solution, whereas the hydrophobic groups are buried inside and have essentially no contact with the water; the corresponding free-energy change has a large entropic contribution arising from the configurational entropy of the hydrogen bond networks in the water.

Internal Membranes: Biomembranes within the cell that cover many intracellular organelles such as the cell nucleus, the endoplasmic reticulum, mitochondria, etc.

Lipids: Amphiphilic molecules for which the hydrophobic part consists of two hydrocarbon chains and the hydrophilic part consists of a polar head group.

Lyotropic Liquid Crystal: Liquid crystals that can be swollen by the addition of solvent. In the present context, these liquid crystals consist of stacks of bilayer membranes.

Monolayer: Monomolecular layer of amphiphilic molecules that can be found, e.g., at the interface between two immiscible liquids such as water and oil.

Optical Tweezers: Light trap with a linear size of about 0.5 μm, which is generated by a focused laser beam and which can be used to grasp and to move a single lipid membrane or a whole bunch of membranes.

Plasma Membrane: Biomembrane that represents the boundary between a biological cell and its environment; it consists of a lipid bilayer with many anchored proteins.

Polymer-Induced Curvature: Polymers that are anchored onto the membrane exert entropic forces that induce a "spontaneous" curvature of the decorated membrane.

Shape Fluctuations: Membranes flicker and thus undergo thermally excited undulations that are directly visible in the optical microscope.

Shape Transformations: The shape of vesicles can be transformed in a controlled way by changing the temperature or the osmotic conditions. Such shape transformations can occur in a continuous or discontinuous fashion.

Surfactants: Amphiphilic molecules for which the hydrophobic part usually consists of one hydrocarbon chain.

Tension of Rupture: Lateral tension, of the order of a few mJ/m^2, at which the lipid membrane ruptures.

Unbinding Transition: Phase transition of interacting membranes between a bound adhesive state at low temperatures and an unbound nonadhesive state at high temperatures.

Vesicle: Closed bilayer without edges, which can attain a large variety of different shapes. An onionlike structure consisting of several closed bilayers is usually called a liposome.

Works Cited

Alberts, B., Bray, D., Lewis, J., Raff, J. M., Roberts, K., Watson, J. D. (1994), *Molecular Biology of the Cell,* 3rd ed., New York: Garland.

Bar-Ziv, R., Menes, R., Moses, E., Safran, S.-A. (1995), *Phys. Rev. Lett.* **75,** 3356-3359.

Brochard, F., Lennon, J. F. (1975), *J. Phys. (Paris)* **36,** 1035-1047.

Canham, P. B. (1970), *J. Theoret. Biol.* **26,** 61-81.

Cevc, C., Marsh, D. (1987), *Phospholipid Bilayers: Physical Principles and Models,* New York: Wiley.

Chassy, B. M., Saunders, J. A., Sowers, A. E. (Eds.) (1992), *Guide to Electroporation and Electrofusion,* San Diego: Academic.

Darnell, J., Lodish, H., Baltimore, D. (1990), *Molecular Cell Biology. Scientific,* New York: W. H. Freeman.

de Gennes, P.-G., Taupin, C. (1982), *J. Phys. Chem.* **86,** 2294-2304.

Evans, E. A. (1974), *Biophys. J.* 14, 923-931.

Evans, E., Needham, D. (1987), *J. Phys. Chem.* **91,** 4219-4228.

Farge, E., Devaux, P. F. (1992), *Biophys. J.* **61,** 347-357.

Goldstein, R. E., Nelson, P., Powers, T., Seifert, U. (1996), *J. Phys. II (France)* **6,** 767-796.

Gompper, G., Kroll, D. M. (1995), *Phys. Rev. E* 51, 514-525.

Helfrich, W. (1973), *Z. Naturforsch.* **28c,** 693-703.

Helfrich, W. (1978), *Z. Naturforsch.* **33a,** 305-315.

Helfrich, W. (1989), *Liquid Cryst.* **5,** 1647-1658.

Hiergeist, C., Lässig, M., Lipowsky, R. (1994), *Europhys. Lett.* **28,** 103-108.

Israelachvili, J. N., Wennerström, H. (1990), *Langmuir* **6,** 873-876.

Jülicher, F., Lipowsky, R. (1996), *Phys. Rev. E* **53,** 2670-2683.

Jülicher, F., Seifert, U., Lipowsky, R. (1993), *Phys. Rev. Lett.* **71,** 452-455.

Kahlweit, M., Lipowsky, R. (Eds.) (1996), *Microemulsions—Experiment and Theory,* Berichte der Bunsengesellschaft für Physikalische Chemie No. 100, 181-393.

König, S., Pfeiffer, W., Bayerl, T., Richter, D., Sackmann, E. (1992), *J. Phys. II (France)* **2,** 1589-1615.

Krstic, R. V. (1976), *Ultrastruktur der Säugetierzelle,* Berlin: Springer.

Lasic, D. D. (1993), *Liposomes: From Physics to Applications,* Amsterdam: Elsevier.

Lasic, D. D. (1994), *Angew. Chem. Int. Ed. Engl.* **33,** 1685-1698.

Lipowsky, R. (1991), *Nature* **349,** 475-481.

Lipowsky, R. (1995a), *Z. Phys. B* **97,** 193-203.

Lipowsky, R. (1995b), *Curr. Opin. Struct. Biol* **5,** 531-540.

Lipowsky, R., Grotehans, S. (1994), *Biophys. Chem.* **49,** 27-37.

Lipowsky, R., Leibler, S. (1986), *Phys. Rev. Lett.* **56,** 2541-2544.

Marcelja, S., Radic, N. (1976), *Chem. Phys. Lett.* **42,** 129-130.

Marra, J., Israelachvili, J. N. (1985), *Biochemistry* 24, 4608-4618.

McIntosh, T. J., Simon, S. A. (1993), *Biochemistry* **32,** 8374-8384.

McIntosh, T. J., Magid, A. D., Simon, S. A. (1989), *Biochemistry* **28,** 7904-7912.

Meunier, J., Langevin, D., Boccara, N. (Eds.) (1987), *Physics of Amphiphilic Layers,* Springer Proceedings in Physics vol. 21, Berlin: Springer.

Miao, L., Seifert, U., Wortis, M., Döbereiner, H.-G. (1994), *Phys. Rev. E* **49,** 5389-5407.

Michalet, X., Bensimon, D. (1995), *Science* **269,** 666-668.

Mutz, M., Helfrich, W. (1989), *Phys. Rev. Lett.* **62,** 2881-2884.

Nelson, D., Piran, T., Weinberg, S. (Eds.) (1989), *Statistical Mechanics of Membranes and Surfaces,* Singapore: World Scientific.

Netz, R. R., Lipowsky, R. (1993), *Phys. Rev. Lett.* **71,** 3596-3599.

Neumann, E., Sowers, A. E., Jordan, C. A. (Eds.) (1989), *Electroporation and Electrofusion in Cell Biology,* New York: Plenum Press.

Pastor, R. W. (1994), *Curr. Opin. Struct. Biol.* **4,** 486-492.

Rädler, J., Feder, T. J., Strey, H. H., Sackmann, E. (1995), *Phys. Rev. E* **51,** 4526-4536.

Rand, R. P., Parsegian, V. A. (1989), *Biochim. Biophys. Acta* **988,** 351-376.

Sackmann, E. (1990), *Can. J. Phys.* **68,** 999-1012.

Seifert, U., Lipowsky, R. (1995), in: R. Lipowsky, E. Sackmann (Eds.), *Handbook of Biological Physics,* Vol. 1, *The Structure and Dynamics of Membranes,* Amsterdam: Elsevier.

Simon, J., Kühner, M., Ringsdorf, H., Sackmann, E. (1995), *Chem. Phys. Lipids* **76,** 241-258.

Tanford, C. (1991), *The Hydrophobic Effect: Formation of Micelles and Biological Membranes,* Malabar, FL: Krieger.

Wiener, C. M., White, S. H. (1992), *Biophys. J.* **61,** 434-447.

Willmore, T. J. (1982), *Total Curvature in Riemannian Geometry,* Chichester: Ellis Horwood.

Further Reading

Bloom, M., Evans, E., Mouritsen, O. G. (1991), *Quart. Rev. Biophys.* **24,** 293-397.

Cevc, C., Marsh, D. (1987), *Phospholipid Bilayers: Physical Principles and Models,* New York: Wiley.

Chassy, B. M., Saunders, J. A., Sowers, A. E. (Eds.) (1992), *Guide to Electroporation and Electrofusion,* San Diego: Academic.

Gennis, R. (1989), *Biomembranes: Molecular Structure and Function,* New York: Springer-Verlag.

Lasic, D. D. (1993), *Liposomes: From Physics to Applications,* Amsterdam: Elsevier.

Lipowsky, R., Sackmann, E. (Eds.) (1995), *Handbook of Biological Physics,* Vol. 1, *Structure and Dynamics of Membranes,* Amsterdam: North-Holland.

Seifert, U. (1997), "Configurations of Fluid Vesicles and Membranes," *Adv. Phys.* **46,** 13-137.

Shinitzky, M. (Ed.) (1993), *Biomembranes: Physical Aspects,* New York: VCH Publishers.